Middle East Journal of Applied Sciences
Volume: 15 | Issue: 03| July – Sept. | 2025

EISSN: 2706 -7947 ISSN: 2077- 4613
DOI: 10.36632/mejas/2025.15.3.15
Journal homepage: www.curresweb.com
Pages: 179-188

Transition-Metal-Enhanced Hydrogen Adsorption on CNNCs: A DFT Analysis

M. A. Al-Khateeb[1] and A. A. EL-Barbary[2]

[1]Physics Department, Faculty of Education and Science, Taiz University, Taiz, Yemen.
[2]Department of Physical Sciences, Physics Division, College of Science, Jazan University, P.O. Box. 114, Jazan, 45142, Kingdom of Saudi Arabia.

Received: 20 June 2025 **Accepted:** 25 August 2025 **Published:** 10 Sept. 2025

ABSTRACT

Due to Growing concerns regarding fossil fuel depletion and the environmental impact of their high consumption necessitate intensified research into renewable and clean alternatives, such as hydrogen, to meet Department of Energy (DOE) targets. In this study, the density functional theory calculations applying 6-31g(d,p) at B3LYP level comprehensively investigate carbon nanocones (CNCs) doped with Cu, Ti, Zn, and V. The analysis encompasses the electronic properties of structures featuring two disclination angles as a function of nanocones size. Furthermore, the mechanism of monohydrogen atom adsorption onto these doped CNC systems is examined. Computational results identify the V-doped $C_{75}H_9$ structure with a 300° disclination angle as the most promising candidate for hydrogen storage. Additionally, the adsorption of hydrogen is found to reduce the electronic band gap energy. These findings collectively indicate that doped carbon nanocones represent a viable candidate material for hydrogen storage applications.

Keywords: CNCs, DFT, hydrogen storage, density functional theory, surface reactivity.

1. Introduction

Nanotechnology continues to reshape modern science and engineering, primarily through innovations at the atomic and molecular scale. One of the most impactful developments has been the rise of nanomaterials, which are tailored to address increasing demands for smaller, faster, and more energy efficient technologies. A prominent class within this field is carbon based nanostructures (Iijima, 1991; Garberg *et al.,* 2008; El-Barbary, 2016a; El-Barbary *et al.,* 2015; Shalabi *et al.,*1998; EL-Barbary and Al-Khateeb, 2021; Savini *et al.,* 2007; Al Roman *et al.,* 2024; Al-Khateeb and El-Barbary, 2018; Shalabi *et al.,* 1999; El-Barbary, 1999; El-Barbary *et al.,* 2010; El-Barbary *et al.,* 2006; Heggie *et al.,* 2007; El-Barbary *et al.,* 2008). Since the discovery of carbon nanotubes (CNTs) in the early 1990 (Iijima, 1991), these cylindrical carbon arrangements have drawn attention for their remarkable strength, electrical conductivity, and heat resistance. More recently, attention has expanded to include carbon nanocones (CNCs) conical analogues of CNTs that share many of their advantageous properties while offering unique geometrical features that may be exploited in precision nanoscale engineering (Heggie *et al.,* 2004; Sattler, 1995; El-Barbary, 2025; El-Barbary *et al.,* 2025; El-Barbary, 2024; EL-Barbary and Adawi, 2024; El-Barbary and Shabi, 2024; El-Barbary, 2023). Simultaneously, silicon carbide (SiC) has emerged as a cornerstone material for extreme operational environments. Its crystalline framework consists of covalently bonded silicon and carbon atoms arranged in a tetrahedral sp^3 hybridized lattice, with uniform interatomic distances of ~3.08 Å across polytypes (Al-Khateeb *et al.,* 2023; El-Barbary and Al-Dosari, 2023). This structural rigidity underpins SiC's exceptional thermal stability, radiation resistance, and mechanical hardness, making it ideal for aerospace and high-energy systems. While SiC nanotubes have been rigorously studied for their resilience under stress and heat (Harris, 1995; Zetterling, 2002; Wu and Guo, 2007), silicon carbide nanocones (SiCNCs) remain underexplored despite their theoretical utility (Matsunami., 2004). This oversight is notable given empirical evidence that conical nanostructures enhance light-trapping efficiency in photovoltaics (Gali,

Corresponding Author: M. A. Al-Khateeb, Physics Department, Faculty of Education and Science, Taiz University, Taiz, Yemen. E-mail: m_alkhateeb77@yahoo.com

2006), a critical advantage for extraterrestrial solar arrays exposed to intense radiation, thermal extremes, and variable solar flux.

Parallel advancements in energy storage have spotlighted nanostructured carbon materials as viable substrates for hydrogen containment. CNTs, graphene derivatives, and porous carbon matrices are under investigation for their adsorption capacities, leveraging high surface-area-to-volume ratios and tunable pore architectures (Alfieri and Kimoto, 2009; Mavrandonakis *et al.,* 2006; Zhu *et al.,* 2009; El-Barbary, 2019; El-Barbary, 2016b; El-Barbary, 2018; El-Barbary, 2015; EL-Barbary and Hindi, 2015; EL-Barbary, 2017; EL-Barbary *et al.,* 2007; EL-Barbary, 2016c).

CNTs, with their hollow cylindrical morphology and low mass density, enable efficient hydrogen physisorption and chemisorption, offering scalable solutions for vehicular fuel storage (EL-Barbary, 2015; Berry and Aceves, 1998; Chen *et al.,* 1998). Storage dynamics in these systems are intrinsically temperature-dependent, permitting precise control over hydrogen uptake and release (Liu and Cheng, 2005; Strobel *et al.,* 2006). Recent mechanistic insights reveal that hydrogen storage involves catalytic dissociation of H_2 molecules at metal nanoparticle sites (often residual from synthesis), followed by atomic hydrogen migration onto the carbon scaffold (Baughman *et al.,* 2002; Yang and Yang, 2002; Zhao *et al.,* 2005; Yang *et al.,* 2006). This process underscores the synergistic role of catalytic impurities and nanomaterial design in optimizing storage efficiency, guiding future innovations in clean energy infrastructure.

In this work we investigate carbon nanocones (CNCs) with 60° and 300° disclination angles, both pure and doped Cu, Ti, Zn, and V as potential hydrogen storage materials. Computational analyses focus on adsorption energies, HOMO-LUMO gaps, density of states (DOS), and surface reactivity. By probing these properties, we aim to elucidate the mechanisms by which Cu, Ti, Zn, and V dopants enhances hydrogen storage capacity in nanocones architectures, advancing their viability for energy applications.

2. Methods

DFT calculations used the B3LYP functional (Becke 3-parameter hybrid) with the B3 correlation, employing the 6-31G (d,p) basis set in Gaussian 09W and Gauss View 5 facilitated visualization (Becke., 1993; Vosko *et al.,* 1980; Frisch *et al.,* 2010; Frisch *et al.,* 2009). DOS and Fermi levels were computed with Gauss Sum 2.2.5 (O'Boyle *et al.,* 2008). The study focuses on doped CNNCs and mono-hydrogenated versions, using Cu, Ti, Zn, and V dopants at 60° and 300° disclination angles; fully optimized structures are shown in Figures 1 and 2.

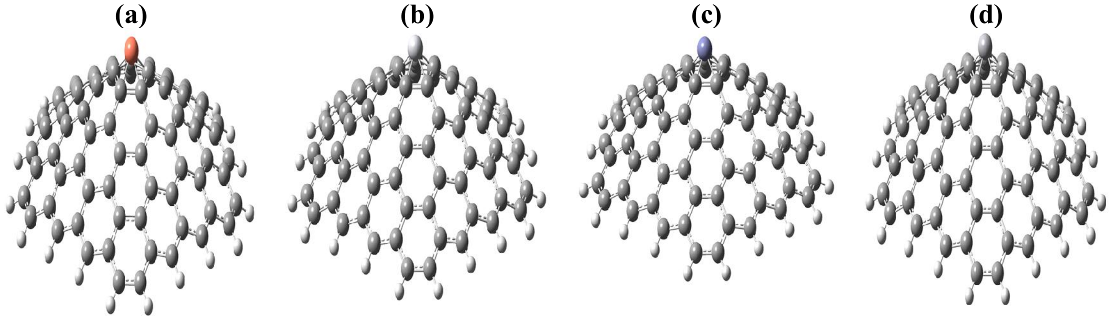

Fig. 1: The fully optimized structures of doped nanocones with disclination angle 60˚ (a) $C_{80}H_{20}$ -Cu, (b) $C_{80}H_{20}$ -Ti, (c) $C_{80}H_{20}$ -Zn, (d) $C_{80}H_{20}$ -V, yellow atom represent copper atom, gray atom represent titanium atom, blue atom represent zinc atom, and silver atom represent vanadium atom.

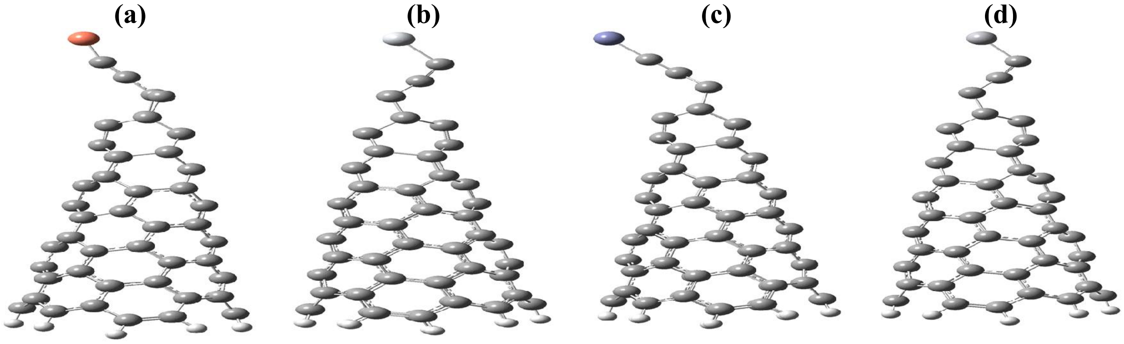

Fig: 2: The fully optimized structures of doped nanocones with disclination angle 300˚ (a) $C_{75}H_9$ -Cu, (b) $C_{75}H_9$ -Ti, (c) $C_{75}H_9$ -Zn, (d) $C_{75}H_9$ -V, yellow atom represent copper atom, gray atom represent titanium atom, blue atom represent zinc atom, and silver atom represent vanadium atom.

3. Results and Discussion

3.1. Adsorption Energy

To enhance carbon nanocones (CNCs) for hydrogen storage, hydrogen adsorption on doped metal CNCs was investigated. Fully optimized configurations for hydrogen adsorption on Cu, Zn, Ti, and V-doped CNCs with disclination angles of 60° and 300° were examined for $C_{80}H_{20}$ and $C_{75}H_9$, respectively, with results presented in Figure 3 and Figure 4. The hydrogen adsorption energy, (E^H_{ads}), for doping CNCs with angles 60° and 300° was calculated as:

$$E^H_{ads} = E_{(NCs\text{-}H)} - E_{(NCs)} - E_{(H)}$$

where ($E_{CNCs\text{-}H}$) is the energy of the optimized mono-hydrogenated doped CNCs, (E_{CNCs}) is the energy of the optimized doped CNCs, and (E_H) is the energy of a hydrogen atom.

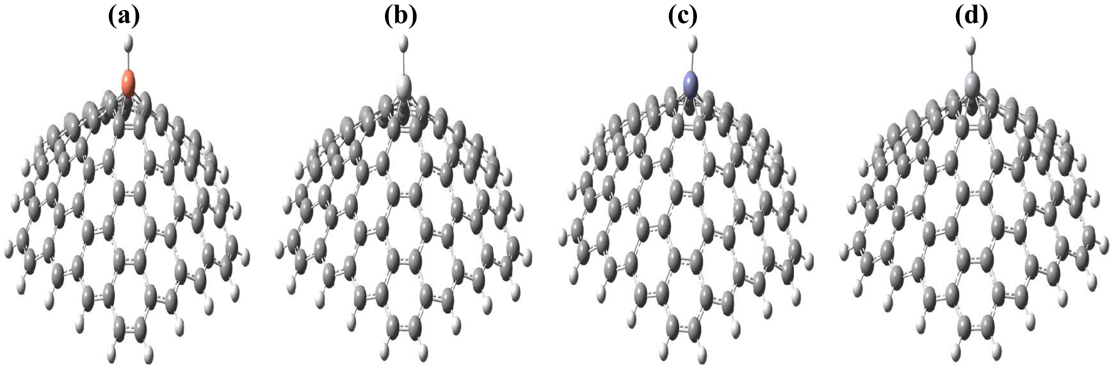

Fig. 3: The fully optimized structures of hydrogen adsorption on the doped nanocones with disclination angle 60˚ (a) $C_{80}H_{20}$ -Cu, (b) $C_{80}H_{20}$ -Ti, (c) $C_{80}H_{20}$ -Zn, (d) $C_{80}H_{20}$ -V, yellow atom represent copper atom, gray atom represent titanium atom, blue atom represent zinc atom, and silver atom represent vanadium atom.

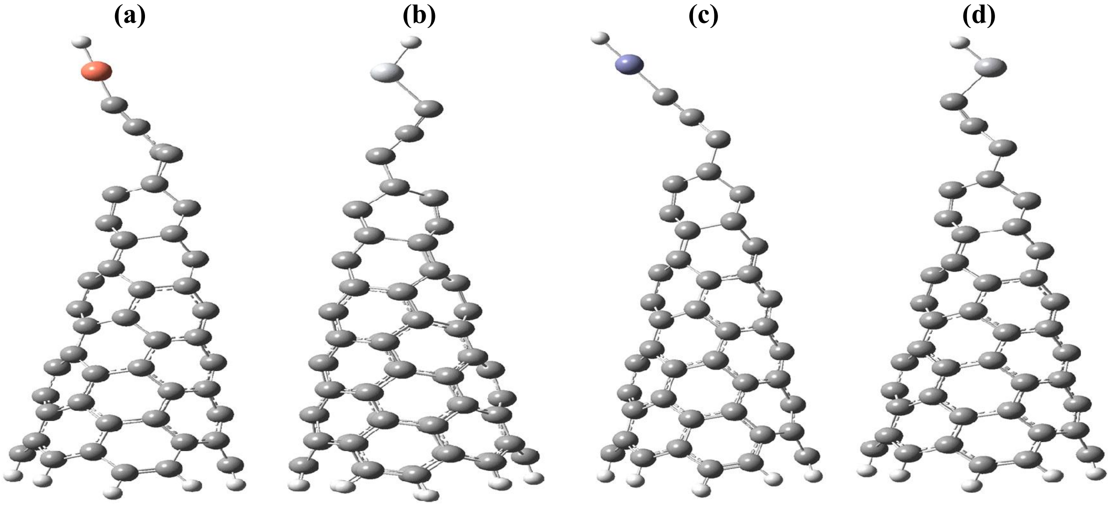

Fig. 4: The fully optimized structures of hydrogen adsorption on the doped nanocones with disclination angle 300˚ (a) $C_{75}H_9$ -Cu, (b) $C_{75}H_9$ -Ti, (c) $C_{75}H_9$ -Zn, (d) $C_{75}H_9$ -V, yellow atom represent copper atom, gray atom represent titanium atom, blue atom represent zinc atom, and silver atom represent vanadium atom.

Similarly, the hydrogen adsorption energy for doped Cu, Ti, Zn, and V at 60° and 300° is obtained from the energy difference between the optimized hydrogenated doped CNCs and the sum of the energies of the doped CNCs and the hydrogen atom. The adsorption energies for disclination angles of 60° and 300° are shown in Table 1. The hydrogen adsorption of pure CNCs with disclination angle 300° (-4.27 eV) is more favorable than those with disclination angle 60° (-2.13 eV). We also assess the hydrogen storage potential of Cu, Ti, Zn, and V-doped CNCs by their adsorption energies. From Table 1, the strongest adsorption energies are −7.22 eV and −6.07 eV for mono-hydrogenated Cu- and Zn-doped $C_{75}H_9$ with a 300° disclination angle. Notably, for all mono-hydrogenated Cu, Ti, Zn, and V-doped $C_{75}H_9$ with a 300° disclination angle, the adsorption energies are consistently lower (more favorable) than those for mono-hydrogenated Cu and Zn-doped $C_{80}H_{20}$ with a 60° disclination angle. One can conclude that doping CNCs with Cu, Ti, Zn, or V is likely to enhance hydrogen storage, consistent with recent graphene/dopant studies (Alshareef, 2020). The most favorable system is $C_{75}H_9$–Cu at 300°, due to curvature effects and carbon properties with potential for microelectronics, optoelectronics, and nanocomposites (El-Barbary, 2019; El-Barbary, 2016a; El-Barbary, 2018; El-Barbary, 2015; EL-Barbary and Hindi, 2015; EL-Barbary, 2017; EL-Barbary *et al.,* 2007; EL-Barbary, 2016c; EL-Barbary, 2016d).

Table 1: The calculated adsorption energy (E^H_{ads})of hydrogenated doped Cu, Ti, Zn, V-CNCs, with disclination angles 60˚ and 300˚. All energies are given by eV.

Angle 60˚	E^H_{ads} **(eV)**	**Angle 300˚**	E^H_{ads} **(eV)**
$\mathbf{C_{80}H_{20}}$	-2.13	$C_{75}H_9$	-4.27
$\mathbf{C_{80}H_{20}}$ **- Cu**	-3.23	$C_{75}H_9$ - Cu	-7.22
$\mathbf{C_{80}H_{20}}$ **- Ti**	-2.73	$C_{75}H_9$ - Ti	-4.31
$\mathbf{C_{80}H_{20}}$ **- Zn**	-2.16	$C_{75}H_9$ - Zn	-6.07
$\mathbf{C_{80}H_{20}}$ **- V**	-2.61	$C_{75}H_9$ - V	-5.09

3.2. Surface Reactivity

The surface reactivity of both pure and hydrogenated Cu, Ti, Zn, and V-doped CNNCs with disclination angles of 60° ($C_{80}H_{20}$) and 300° ($C_{75}H_9$) was analyzed, with dipole moments calculated as indicators of surface reactivity (El-Nahass *et al.,* 2013; Kotz *et al.,* 2006) and summarized in Table 2. Higher dipole moments generally correspond to higher surface reactivity, and surface reactivity increases with different dopants and larger disclination angles, since increasing the nanocone surface area via dopant type and disclination angle can enhance the rate of chemical reactions, suggesting more hydrogen adsorption on the surface. Mono-hydrogenated CNNCs show enhanced reactivity with diverse dopants and larger disclination angles, and among hydrogenated systems, $C_{75}H_9$–Cu with a 300° disclination angle exhibits the highest reactivity (dipole moment = 25.31 Debye) while $C_{80}H_{20}$–V with a 60° disclination angle shows the lowest reactivity (dipole moment = 8.56 Debye); overall. The surface reactivity for mono-hydrogenated CNNCs increases with doping type and disclination angle, and hydrogenation further enhances reactivity, with the peak value observed for $C_{75}H_9$–Cu under hydrogenation on the doped atom, in agreement with previous experimental findings that curvature enhances hydrogen storage capacity in nanotubes (over 7 wt %) due to reversible hydrogen bonds (Nikitin *et al.,* 2008).

Table 2: The dipole moments of hydrogenated doped Cu, Ti, Zn, V-CNCs, with disclination angles 60˚ and 300˚. The dipole moment is given by Debye.

Angle 60˚	Dipole moment (Debye)	Angle 300˚	Dipole moment (Debye)
$C_{80}H_{20}$	1.84	$C_{75}H_9$	4.52
$C_{80}H_{20}$ - Cu	11.78	$C_{75}H_9$ - Cu	25.31
$C_{80}H_{20}$ - Ti	10.64	$C_{75}H_9$ - Ti	16.26
$C_{80}H_{20}$ - Zn	9.07	$C_{75}H_9$ - Zn	17.48
$C_{80}H_{20}$ - V	8.56	$C_{75}H_9$ - V	10.35

3.3. Energy Gap and Molecular Orbitals

The energy gaps of hydrogenated Cu, Ti, Zn, and V-doped CNNCs were examined including $C_{80}H_{20}$ with a 60° disclination and $C_{75}H_9$ with a 300° disclination (Table 3). Zn-doped $C_{80}H_{20}$ consistently shows smaller gaps than the Ti, Cu, or V counterparts. The smallest and largest gaps are 0.01 eV ($C_{75}H_9$–Zn, 300°) and 0.07 eV ($C_{80}H_{20}$–V, 60°), respectively. In addition, it can be reported that the consistent reduction in energy gaps following hydrogen adsorption compared to the pre-adsorption state was observed, aligning with established findings (EL-Barbary, 2016d; EL-Barbary, 2015). Figure 5 shows a positive correlation between the disclination angle and surface chemical reactivity. This enhancement arises because larger disclination angles induce greater structural strain within the nanocones, consequently elevating reactivity.

Table 3: The energy gaps of hydrogenated doped Cu, Ti, Zn, V-CNCs, with disclination angles 60˚ and 300˚. The energy gap is given by eV.

Angle 60˚	E.g (eV)	Angle 300˚	E.g (eV)
$C_{80}H_{20}$	0.07	$C_{75}H_9$	0.02
$C_{80}H_{20}$ - Cu	0.06	$C_{75}H_9$ - Cu	0.05
$C_{80}H_{20}$ - Ti	0.05	$C_{75}H_9$ - Ti	0.01
$C_{80}H_{20}$ - Zn	0.02	$C_{75}H_9$ - Zn	0.02
$C_{80}H_{20}$ - V	0.07	$C_{75}H_9$ - V	0.05

Doping atoms also significantly influence the system by locally augmenting electron density around their lattice sites. This increased electron density facilitates stronger hydrogen adsorption interactions and improves hydrogen storage potential. Consequently, the results demonstrate that the storage capacity of hydrogen, particularly in the $C_{75}H_9$ structure, increases with a greater disclination angle and the incorporation of dopant atoms into the nanocones lattice. These findings are consistent with prior research (Al-Khateeb *et al*., 2023; Zhu *et al*., 2009; Al-Khateeb and El-Barbary., 2020; Savini *et al.,* 2007).

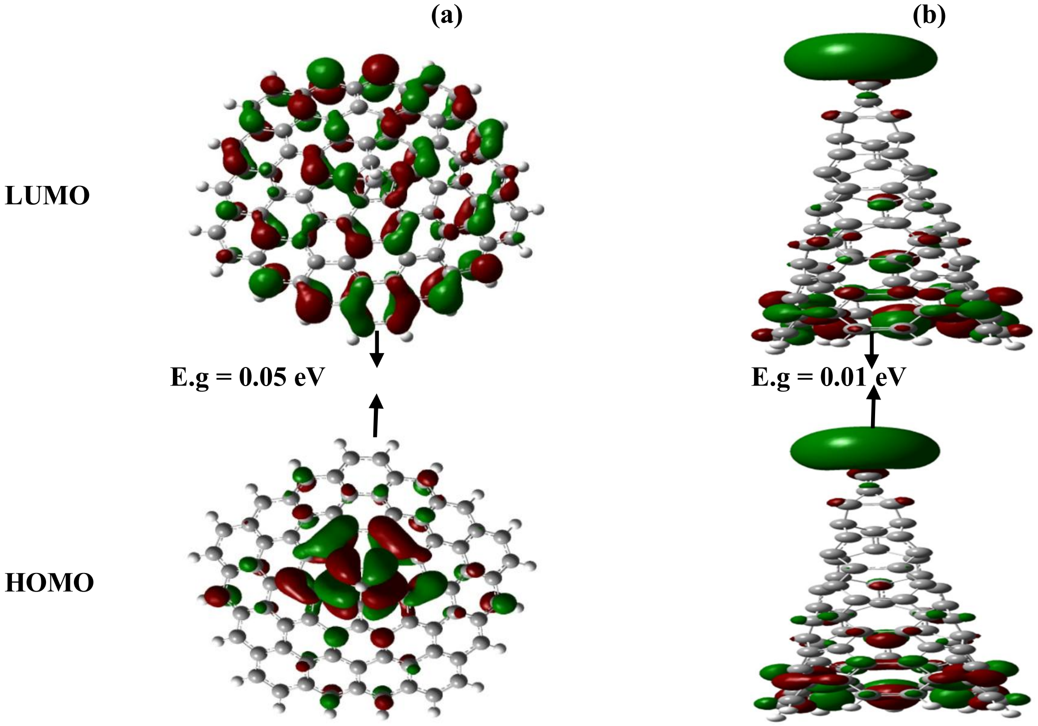

Fig. 5: The molecular orbital of LUMOs and HOMOs for hydrogenated doped Ti-CNCs (a) $C_{80}H_{20}$-Ti with disclination angle 60 and (b) $C_{75}H_9$-Ti with disclination angle 300˚.

4. Conclusion

We have computational analysis via Density Functional Theory (DFT) was employed to investigate the adsorption energetics and electronic structure of hydrogenated carbon nanocones (CNCs). It is found the calculations reveal an inverse relationship between hydrogen adsorption strength and CNC size/disclination angle. Specifically, the system exhibiting the strongest adsorption (most negative adsorption energy of (-7.22 eV) was the mono-hydrogenated $C_{75}H_9$ nanocones doped with Copper (Cu) and possessing a 300˚ disclination angle. Furthermore, a systematic difference in electronic band gaps was observed based on the dopant site for hydrogen adsorption. Mono-hydrogenation at titanium (Ti) dopant sites consistently resulted in smaller band gaps compared to hydrogenation at (Cu, Zn, V) dopant sites. The smallest calculated band gap (0.01 eV) occurred for the Ti-doped $C_{75}H_9$ system with a 300˚ disclination angle. Finally, Hydrogenation was found to enhance surface reactivity, quantified by the dipole moment. The highest reactivity (25.31 Debye) was calculated for the Copper (Cu)-doped $C_{75}H_9$ nanocones when hydrogen was adsorbed onto a Copper (Cu) dopant atom. The high specific surface area inherent to doped CNC structures is a critical factor for their potential application in hydrogen storage devices. This property enables the design of lightweight storage systems with improved hydrogen uptake characteristics. Consequently, further investigation is warranted to explore the capabilities of doping CNCs in key physicochemical processes relevant to hydrogen storage, such as detailed surface interactions and hydrogen dissociation mechanisms.

References

Al Roman, A., H. Adawi, A.A. EL Barbary, M.M. Masud, and M.M. Rahman, 2024. A first-principles investigation of structural, thermodynamic, electronic, and optical properties of doped 2D ZrNI monolayer, Materials Chemistry and Physics, 129268. https://doi.org/10.1016/j.matchemphys.2024.129268

Alfieri, G. and T. Kimoto, 2009. The Structural and Electronic Properties of Chiral SiC Nanotubes: A Hybrid Density Functional Study. Nanotechnology, 20, Article ID: 285703. https://doi.org/10.1088/0957-4484/20/28/285703

Al-Khateeb, M.A. and A.A. El-Barbary, 2018. A Theoretical Study of Hydrogen Adsorption on Surface Nanocone Materials. Current Science International, 7: 370-375. https://www.curresweb.com/csi/csi/2018/370-375

Al-Khateeb, M.A. and A.A. El-Barbary, 2020. Hydrogen Adsorption Mechanism of SiC Nanocones. Graphene, 9, 1-12. https://doi.org/10.4236/graphene.2020.91001

Al-Khateeb, M.A., A.A. El-Barbary, M.A. Kamel, and K.M. Eid, 2023. Vacancy Defects in Carbon Nanotubes for Hydrogen Storage, M.A. Al-Khateeb, A. A. El-Barbary, M. A., Kamel, K.M. Eid, Current Science International, 12. https://www.curresweb.com/index.php/CSI1/article/view/303

Alshareef, B., 2020. DFT Investigation of the Hydrogen Adsorption on Graphene and Graphene Sheet Doped with Osmium and Tungsten. Open Journal of Physical Chemistry, 10: 197-204. https://doi.org/10.4236/ojpc.2020.104012

Baughman, R.H., A.A. Zakhidov, and W.A. De Heer, 2002. Carbon Nano tubes—The Route toward Applications. Science, 297: 787-792. https://doi.org/10.1126/science.1060928

Becke, A.D., 1993. Density-Functional Thermochemistry. III. The Role of Exact Exchange. Chemical Physics, 98: 5648. https://doi.org/10.1063/1.464913

Berry, G.D. and S.M. Aceves, 1998. Onboard Storage Alternatives for Hydrogen Vehicles. Energy Fuels, 12: 49-55. https://doi.org/10.1021/ef9700947

Chen, P., X. Wu, J. Lin, and K.L. Tan, 1999. High H2 Uptake by Alkali-Doped Carbon Nano Tubes under Ambient Pressure and Moderate Temperatures. Science, 285: 91-93.

EL-Barbary, A.A. and A.A. Hindi, 2015. Hydrogen Storage on Halogenated C40 Cage: An Intermediate between Physisorption and Chemisorptions. Journal of Mo lecular Structure, 1080, 169-175. https://doi.org/10.1016/j.molstruc.2014.09.034

El-Barbary, A.A. and A.H. Shabi, 2024. Stone-Wales defective C60 fullerene for hydrogen storage, International Journal of Hydrogen Energy 71: 155-164. https://doi.org/10.1016/j.ijhydene.2024.05.240

EL-Barbary, A.A. and H. Adawi, 2024. Energetic and spectroscopic properties of n-type and p-type C60 fullerene, Diamond and Related Materials, 111266. https://doi.org/10.1016/j.diamond.2024.111266

El-Barbary, A.A. and I.F.M. Al-Dosari, 2023. New insights into electronic and adsorption energies of metallofullerenes C19M, Results in Materials 19: 100428. https://doi.org/10.1016/j.rinma.2023.100428

EL-Barbary, A.A. and M.A. Al-Khateeb, 2021. DFT study of Se-doped nanocones as highly efficient hydrogen storage carrier, Graphene, 10 (4): 49-60. https://doi.org/10.4236/graphene.2021.104004

El-Barbary, A.A., 1999. Vacancy cluster in graphite: Migration energy and aggregation mechanism, AIP Conference Proceedings, 1976 (1): 02006.

EL-Barbary, A.A., 2015. 1H and 13C NMR Chemical Shift Investigations of Hydro genated Small Fullerene Cages Cn, Cn H, Cn Hn and Cn Hn+1 : n=20, 40, 58, 60. Journal of Molecular Structure, 1097: 76-86. https://doi.org/10.1016/j.molstruc.2015.05.015

EL-Barbary, A.A., 2015. The Surface Reactivity and Electronic Properties of Small Hydrogenation Fullerene Cages. Journal of Surface Engineered Materials and Advanced Technology, 5: 162-168. https://doi.org/10.4236/jsemat.2015.53018

EL-Barbary, A.A., 2016a. Potential Energy of H2 inside the C116 Fullerene Dimerization: An Atomic Analysis. Journal of Molecular Structure, 1112: 9-13. https://doi.org/10.1016/j.molstruc.2016.02.007

EL-Barbary, A.A., 2016b. Hydrogenated Fullerenes Dimer, Peanut and Capsule: An Atomic Comparison. Applied Surface Science, 369: 50-57. https://doi.org/10.1016/j.apsusc.2016.02.033

EL-Barbary, A.A., 2016c. Hydrogenated Fullerenes in Space: FT-IR Spectra Analysis. AIP Conference Proceedings, 1742, Article ID: 030005. https://doi.org/10.1063/1.4953126

EL-Barbary, A.A., 2016d. Hydrogenation Mechanism of Small Fullerene Cages. International Journal of Hydrogen Energy, 41, 375-383. https://doi.org/10.1016/j.ijhydene.2015.10.102

EL-Barbary, A.A., 2017. New Insights into Canted Spiro Carbon Interstitial in Graphite. Applied Surface Science, 426: 238-243. https://doi.org/10.1016/j.apsusc.2017.07.196

EL-Barbary, A.A., 2018. Vacancy Cluster in Graphite: Migration Mechanism and Aggregation. AIP Conference Proceedings, 1976, Article ID: 020006. https://doi.org/10.1063/1.5042373

El-Barbary, A.A., 2019. Hydrogen Storage on Cross Stacking Nanocones. International Journal of Hydrogen Energy, 44, Article ID: 20099. https://doi.org/10.1016/j.ijhydene.2019.05.043

El-Barbary, A.A., 2023. IR spectroscopic analysis of heterohedral metallofullerenes, Diamond and Related Materials 136, 110082. https://doi.org/10.1016/j.diamond.2023.110082

El-Barbary, A.A., 2024. IR spectroscopic and vibrational modes of C59X and C60X fullerenes (X = Li, Be), Diamond and Related Materials 148: 111448. https://doi.org/10.1016/j.diamond.2024.111448

El-Barbary, A.A., 2025. IR spectroscopy insights and sensitivity of fullerene C59Al for pollutant gas detection, Diamond and Related Materials, 112738. https://doi.org/10.1016/j.diamond.2025.112738

El-Barbary, A.A., H.I. Lebda, and M.A. Kamel, 2006. Wigner energy release of clustering vacancy defects irradiated graphite, Conference: RPC-2006.8. Radiation Physics and Protection Conference, Beni Sueif (Egypt): ISSN 1110-0451, CODEN: AJNADV, Special Issue, 40. https://inis.iaea.org/records/hg9ez-4nd79

El-Barbary, A.A., H.I. Lebda, and M.A. Kamel, 2008. Radiation Damage and Dimensional Changes, Conference: RPCXI: 9. Radiation Physics and Protection Conference, Cairo (Egypt): 15-19 Nov 2008. https://www.osti.gov/etdeweb/servlets/purl/21228408

El-Barbary, A.A., H.I. Lebda, and M.A. Kamel, 2009. The High Conductivity of Defect Fullerene C40 Cage. Computational Materials Science, 46: 128-132. https://doi.org/10.1016/j.commatsci.2009.02.034

El-Barbary, A.A., K.M. Eid, M.A. Al-Khateeb, and M.A. Kamel, 2010. The Role of Irradiation in Graphite for Hydrogen Storage. Arab Journal of Nuclear Sciences and Applications. https://inis.iaea.org/collection/NCLCollectionStore/_Public/42/076/42076631.pdf?r=1

El-Barbary, A.A., M.A. Kamel, K.M. Eid, H.O. Taha, and M.M. Hassan, 2015. Mono-vacancy and B-doped defects in carbon heterojunction nanodevices, , Graphene 4(04): 84. https://doi.org/10.4236/graphene.2015.44009

El-Barbary, A.A., S.M. Khurmy, and H. Adawi, 2025. Band Gap Engineering of Nanocones via Mono-Hydrogenation, , Macromolecular Symposia 414 (1): 2400002. https://doi.org/10.1002/masy.202400002

El-Nahass, M.M., M.A. Kamel, A.A. El-Barbary, M.A.M. El-Mansy, and M. Ibrahim, 2013. On the Spectroscopic Analyses of Thioindigo Dye. Spectrochimica Acta Part A: Molecular and Biomolecular Spectroscopy, 113: 332-336.

Frisch, A., R.D. Dennington, T.A. Keith, J. Millam, A.B. Nielsen, A.J. Holder, and J. Hiscocks, 2009. Gauss View Manual Version 5.0.9. Gaussian Inc., Wallingford.

Frisch, M.J., G.W. Trucks, H.B. Schlegel, G.E. Scuseria, M.A. Robb, J.R. Cheeseman, V.G. Zakrzewski, J.A. Montgomery, R.E. Stratmann, J.C. Burant, S. Dapprich, J.M. Millam, A.D. Daniels, K.N. Kudin, M.C. Strain, O. Farkas, J. Tomasi, V. Barone, M. Cossi, R. Cammi, B. Mennucci, C.Pomelli, C. Adamo, S. Clifford, J. Ochterski, G.A. Petersson, P.Y. Ayala, Q. Cui, K. Morokuma, D.K. Malick, A.D. Rabuck, K. Raghavachari, J.B. Foresman, J. Cioslowski, J.V. Ortiz, B.B. Stefanov, G. Liu, A. Liashenko, P. Piskorz, I. Komaromi, R. Gomperts, R.L. Martin, D.J. Fox, T. Keith, M. Al-Lamham, C.Y. Peng, A. Nanayakkara, C. Gonzalez, M. Challacombe, P.M.W. Gill, B.G. Johnson, W. Chen, M.W. Wong, J.L. Andres, M. Head-Gordon, E.S. Replogle, and J.A. Pople, 2010. Gaussian 2010. Gaussian Inc., Wallingford.

Gali, A., 2006. Ab initio Study of Nitrogen and Boron Substitutional Impurities in Single-Wall SiC Nanotubes. Physical Review B, 73, Article ID: 245415. https://doi.org/10.1103/PhysRevB.73.245415

Garberg, S.N., G. Naess, K.D. Helgesen, G. Knudsen, A. Kopstad, and A. Elgsaeter, 2008. Transmission Electron Microscopeand Electron Diraction Study of Carbon Nanodisks, Carbon, 46: 1535-1543. https://doi.org/10.1016/j.carbon.2008.06.044

Harris, G.L., 1995. Properties of Silicon Carbide. INSPEC, the Institution of Electrical Engineers, London.

Heggie, M., I. Suárez-Martínez, G. Savini, A.A. El-Barbary, C. Ewels, and R. Telling, 2007. Irradiation damage in graphite from first principles, Special Publication-Royal Society Of Chemistry 309, 83. https://doi.org/10.1103/PhysRevLett.98.015501

Heggie, M., R. Telling, A.A. El-Barbary, I. Suarez-Martinez, and C. Ewels, 2004. Carbon under irradiation-stiffening, creeping and shape change, Conference: 6. international conference on Nano-technology in Carbon: from synthesis to applications of nano-structured carbon and related materials, Batz sur Mer (France): 10-13 Oct 2004.

Iijima, S., 1991. Helical Microtubules of Graphitic Carbon, Nature, 354: 56-58. https://doi.org/10.1038/354056a0

Kotz, J.C., P. Treichel, and G.C. Weaver, 2006. Chemistry and Chemical Reactivity. Thomson Brooks Cole, Pacific Grove.

Liu, C. and H.M. Cheng, 2005. Carbon Nanotubes for Clean Energy Applications. Journal of Physics D: Applied Physics, 38: 231-252. https://doi.org/10.1088/0022-3727/38/14/R01

Matsunami, H., 2004. Technological Breakthroughs in Growth Control of Silicon Carbide for High Power Electronic Devices. Japanese Journal of Applied Physics, 43: 6835. https://doi.org/10.1143/JJAP.43.6835

Mavrandonakis, A., G.E. Froudakis, A. Andriotis, and M. Menon, 2006. Silicon Carbide Nanotube Tips: Promising Materials for Atomic Force Microscopy and/or Scanning Tunneling Microscopy. Physical Review Letters, 89, Article ID: 123126. https://doi.org/10.1063/1.2221418

Nikitin, A., X.L. Li, Z.Y. Zhang, H. Ogasawara, H.J. Dai, and A. Nilsson, 2008. Hydrogen Storage in Carbon Nanotubes through the Formation of Stable C-H Bonds. Nano Letters, 8: 162-167. https://doi.org/10.1021/nl072325k

O'Boyle, N.M., A.L. Tenderholt, K.M. Langer, and J. Chem, 2008. Comput. 29: 839 – 845.

Sattler, K., 1995. Scanning Tunneling Microscopy of Carbon Nanotubes and Nanocones, Carbon, 33: 915-920. https://doi.org/10.1016/0008-6223(95)00020-E

Savini, G., A.A. El Barbary, M.I. Heggie, and S. Öberg, 2007. Partial dislocations under forward bias in SiC, Materials science forum, 556: 279-282. https://www.scientific.net/MSF.556-557.279

Shalabi, A.S., A.M. El-Mahdy, K.M. Eid, M.A. Kamel, and A.A. El-Barbary, 1999. Structure, structural phase transitions, mechanical properties, defects, etc-Glasner-Tompkins relation and reorientation of U centers in LiF crystals, Physical Review-Section B-Condensed Matter 60 (13): 9377-9382. https://doi.org/10.1103/PhysRevB.60.9377

Shalabi, A.S., K.M. Eid, M.A. Kamel, and A.A. El-Barbary, 1998. Comparative study of errors in HeH− interaction energy, calculations, International journal of quantum chemistry, 68 (5): 329-350.

Strobel, R., J. Garche, P.T. Moseley, L. Jorissen, and G. Wolf, 2006. Hydrogen Storage by Carbon Materials. Journal of Power Sources, 159: 781-801. https://doi.org/10.1016/j.jpowsour.2006.03.047

Vosko, S.H., L. Wilk, M. Nusair, and J. Can, 1980. Influence of an Improved Lo cal-Spin-Density Correlation-Energy Functional on the Cohesive Energy of Alkali Metals. Physical Review B, 22: 3812-3815. https://doi.org/10.1103/PhysRevB.22.3812

Wu, J.J. and G.Y. Guo, 2007. Optical Properties of SiC Nanotubes: An Ab initio Study. Physical Review B, 76, Article ID: 035343. https://doi.org/10.1103/PhysRevB.76.035343

Yang, F.H. and R.T. Yang, 2002. Adsorption Behaviors of HiPco Single-Walled Carbon Nanotube Aggregates for Alcohol Vapors. The Journal of Physical Chemi stry, 106: 8994-8999.

Yang, F.H., A.J. Lachawiec, and R.T. Yang, 2006. Hydrogen Sorption on Palla dium-Doped Sepiolite-Derived Carbon Nanofibers. The Journal of Physical Chemi stry B, 110: 6236-6244. https://doi.org/10.1021/jp056461u

Zetterling, C.M., 2002. Process Technology for Silicon Carbide Devices. IET, Lon don. https://doi.org/10.1049/PBEP002E.

Zhao, Y., Y.H. Kim, A.C. Dillon, M.J. Heben, and S.B. Zhang, 2005. Ab initio De sign of Ca-Decorated Organic Frameworks for High Capacity Molecular Hydrogen Storage with Enhanced Binding. Physical Review Letters, 95, Article ID: 155504. https://doi.org/10.1103/PhysRevLett.94.155504

Zhu, J., Z. Yu, G.F. Burkhard, C.M. Hsu, S.T. Connor, Y. Xu, Q. Wang, M. McGe hee, S. Fan, and Y. Cui, 2009. Optical Absorption Enhancement in Amorphous Silicon Nanowire and Nanocone Arrays. Nano Letters, 9: 279-282. https://doi.org/10.1021/nl802886y